PERFORMANCE OF MIMO OFDM SYSTEMS IN FADING CHANNELS

L. Morgoş[*], C. Kokkonis[**]
[*] Department of Electronics,
University of Oradea, Faculty of Electrical Engineering and Information Technology,
1 Universităţii St., 410087, Oradea, Romania, E-Mail:lmorgos@uoradea.ro

[**]Technological Educational Institute of Piraeus, Greece

Abstract ***–The performance of OFDM based systems is seriously affected by imperfections in system implementation. To gain a beter understanding of the influence of these impairments on the performance of multiple antenna OFDM systems, this paper studies a zero-forcing based MIMO OFDM system with imperfections modeled as additive error sources in both transmitter (TX) and receiver (RX). Based on this model, expressions are derived for the probability of error of uncoded impaired MIMO systems in fading and non-fading environments. These results allow for insightful comparison between the influence of TX and RX impairments. It is concluded that the influence of RX imperfections decreases with an increasing number of RX branches, while this is not the case for TX deficiencies.***

I. INTRODUCTION

The application of multiple antennas at both transmitter (TX) and receiver (RX) side of wireless communication systems is proposed in many contributions over the last few years. It provides the benefit of increased range, robustness and/or improved data rate. This class of systems is often named multiple-input multiple-output (MIMO), referring to themulti-dimensional wireless channel. When applying these techniques to wideband communication, the combination of the MIMO architectures with the multicarrier technique orthogonal frequency division multiplexing (OFDM) is promising. The combination, MIMO OFDM, enables the application of the narrowband based MIMO techniques to every subcarrier, separately. The potential of this physical layer approach has led to the numerous proposals in standardization at this moment, based on this concept, e.g., in the Wireless Local-Area-Network (WLAN) group IEEE 802.11.

Research concerningMIMO OFDMbased systemsmainly focusses on systems impaired by additive white Gaussian receiver noise and spatial correlated channels. When implementing such a system, however, many other impairments will arise, which can largely influence the performance of the wireless system. Many publications, e.g., [1], show that the performance of OFDM systems is severely degraded by different kind of implementations imperfections. The influence of phase noise, I/Q imbalance, limited word length due to fixed point implementation, non-lineair power amplifiers, and DC-offset are regarded as the main contributors to bit-error-rate (BER) degradation. One commonly used measure for the aggregate severeness of these imperfections in system design is the errorvector-magnitude (EVM) [2], which basically measures the second moment of the error in the estimated symbols. Another frequently used measure is implementation loss, which indicates the extra signal-to-noise ratio (SNR) necessary to overcome the impairment and achieve the same BER as the non-impaired system. In order to unambiguously relate these measures to the final system performance measure BER, the error term resulting from all implementation deficiencies has to be a zero-mean complex Gaussian process. To enable good design choices using these error measures it is important to first understand how the BER of a system is influenced by these deficiencies and secondly to understand whether and how the different impairments contribute to these error measures. This paper regards the first issue, which is unto now not treated for MIMO systems, and hereto studies the probability of error of a system experiencing TX and RX imperfections. These impairments are here modeled as additive noise sources and will be further referred to as additive impairment (AI). Section 2 derives the system model for a multiple antenna system applying OFDM, which experiences both TX and RX AI. The probability of error for such systems in fading channels is derived in Section 3, which shows there is a difference between the influence of TX and RX AI. Section 4 then provides numerical results, which are compared with results from Monte-Carlo simulations. Finally, conclusions are drawn in Section 5.

II. MIMO OFDM SYSTEM MODEL

Consider a MIMO OFDM system with N_t TX and N_r RX antennas, denoted here as a $N_t \times N_r$ system. Figure1

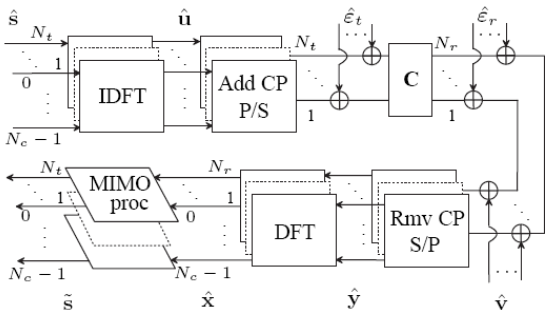

Figure 1: MIMO OFDM baseband system model with additive TX and RX impairments.

depicts the baseband model of such a system. Let us define the MIMO OFDM vector to be transmitted during a symbol period as $\hat{s} = vec(s_0, s_1 ..., s_{N_c - 1})$, where s_n denotes the $N_t \times 1$ frequency domain MIMO transmit vector for the nth subcarrier and N_c represents the number of subcarriers. This vector is transformed to the time domain using the inverse discrete Fourier transform (IDFT). A cyclic prefix (CP) is added to the signal, which adds the last N_t N_g elements $\hat{u}$ on top of $\hat{u}$. We assume here that the CP is at least equal to the channel impulse response (CIR) length, avoiding inter-symbol-interference (ISI). It is, additionally, assumed that the average total TX power is divided among the TX antennas, such that the covariance matrix of $\hat{s} = \sigma_s^2 I$. The signal is then transmitted through the quasi-static multipath channel C. The average channel attenuation is assumed to be 1. At the RX the CP is removed (Rmv CP), and the received signal $\hat{y}$ is converted to the frequency domain using the DFT. This yields

$$\hat{x} = \hat{H}(\hat{s} + \hat{\eta}_t) + \hat{\eta}_r + \hat{n} \qquad (1)$$

where $\hat{H}$ is the $N_c N_r \times N_c N_t$ channel matrix, which is block diagonal since the time domain channel matrix C is block circulant [3]. The nth $N_r \times N_t$ block diagonal element of $\hat{H}$ is H_n, the $N_r \times N_t$ MIMO channel of the nth subcarrier. ˆn represents the frequency-domain noise, with i.i.d. zero-mean, complex Gaussian elements and $\hat{v}$ denotes its time-domain equivalent. The TX and RX impairments are modeled by the additive terms $\hat{\eta}_t$ and $\hat{\eta}_r$, respectively, which are the frequency-domain equivalents of $\hat{\varepsilon}_t$ and $\hat{\varepsilon}_r$ in Fig. 1. Since the channel is block orthogonal, the MIMO processing can be applied per subcarrier, yielding the NcNt × 1 estimate $\tilde{s}$ of the transmitted symbol vector $\hat{s}$. Here we regard a zero-forcing (ZF) receiver, which basically multiplies the received signal $\hat{x}$ with the pseudo-inverse of the channelmatrix $\hat{H}$, which is given by $\hat{H}^{\dagger} = (\hat{H}^H \hat{H})^{-1} \hat{H}^H$.

After ZF-processing the estimate of the transmitted symbol vector is given by

$$\tilde{s} = \hat{H}^{\dagger}\hat{x} = \hat{s} + \eta_t + \hat{H}^{\dagger}(\hat{\eta}_r + \hat{n}) \qquad (2)$$

Note that for the ZF receiver to work Nr ≥ Nt. Furthermore, knowledge about $\hat{H}$ is necessary at the RX. This is generally achieved using pilot-aided channel estimation. For simplicity, however, $\hat{H}$ is here assumed to be perfectly known at the RX.

III. PROBABILITY OF ERROR

The SNR for the ntth branch and the nth subcarrier, affected by a given channel, is now given by

$$\rho = \frac{\sigma_s^2}{\sigma_t^2 + (\sigma_r^2 + \sigma_n^2)\left[(H_n^H H_n)^{-1}\right]_{n_t n_t}} = \frac{1}{\sigma_t^{-1} + N_t(\rho_r^{-1} + \rho_n^{-1})\left[(H_n^H H_n)^{-1}\right]_{n_t n_t}} \qquad (3)$$

where it is assumed that $\hat{\eta}_t$ and $\hat{\eta}_r$ are zero-mean complex Gaussian distributed and that their covariance matrices are given by $\sigma_t^2 I$ and $\sigma_r^2 I$, respectively. Additionally, we assume that the different noise processes are independent. [A]mm denotes the mth diagonal element of matrix A. Furthermore, ρ_n denotes the SNR for a system without system imperfections, i.e., only impaired by additive Gaussian receiver noise. $\rho_t = \sigma_s^2 / \sigma_t^2$ and $\rho_r = N_t \sigma_s^2 / \sigma_r^2$ are the SNR for a system only impaired by TX or RX AI, respectively.

The symbol error rate (SER) for the ntth branch and nth subcarrier of an uncoded system is then found by [4]

$$P_e = \int_0^{\infty} P_{e,M}(\rho) p(\rho) d\rho \qquad (4)$$

where the $P_{e,M}(\rho)$ denotes the approximation of the SER for a M-QAM constellation and is given by $aQ(\sqrt{bp})$. In this expression $a = 4(1 - 1/\sqrt{M})$ and $b = 3/(M-1)$. The average SER is now found by averaging P_e over the different subcarriers and branches. The average BER is then found by dividing the SER by $\log2(M)$. When there is no fading and the MIMO channels are perfectly orthogonal, it is easily seen that $(\hat{H}^H \hat{H})^{-1} = I/N_r$.

In that case the RX noise and AI contribute Nr times less than the TX AI to the total noise in the SNR expression. For this non-fading case the probability of symbol error is then easily found by substituting

$$\rho = \left[\frac{1}{\rho_t} + \frac{N_t}{N_r}\left(\frac{1}{\rho_r} + \frac{1}{\rho_n}\right)\right]^{-1} \qquad (5)$$

into $P_{eM}(\rho)$

Since it is clear from (3) that the influence of TX and RX AI on the SNR is different, we regard two cases for the fading channel: a case with solely TX AI and one with only RX AI. The MIMO channel elements are i.i.d. according to CN(0, 1), also known as Rayleigh fading.

First we regard the case of RX AI and additive receiver noise. This could be the case of a downlink transmission in which the base station is of high quality and the additive impairment of the user terminal is dominant. The SNR ρ_{RX} for the ntth branch and nth subcarrier in (3) is then given by

$$\rho_{RX} = \frac{\rho_r \rho_n}{N_t(\rho_r + \rho_n)\left[\left(H_n^H H_n\right)^{-1}\right]_{n_t n_t}}. \quad (6)$$

It was shown by Kiessling et al. in [5], that _RX is chisquared distributed with $2P = 2(N_r - N_t + 1)$ degrees of freedom. Its pdf is given by

$$p(\rho_{RX}) = \frac{(\rho_{RX}/\rho_0)^{P-1}}{\rho_0 (P-1)!} \exp\left(-\frac{\rho_{RX}}{\rho_0}\right). \quad (7)$$

where ρ_0 is the average SNR, given by $\frac{1}{N_t}\frac{\rho_r \rho_n}{\rho_r + \rho_n}$.

To derive a closed form expression for (4), we use an alternative representation for the Gaussian Q-function [6, p.71]. By substituting this expression and (7) into (4), working out one integral and by change of integration variable, we find that the probability of symbol error is given by

$$P_e = \frac{a}{\pi}\int_0^\infty \int_0^{\pi/2} \exp\left(-\frac{b\rho}{2\sin^2\varphi}\right) d\varphi p(\rho) d(\rho) =$$

$$= \frac{a}{\pi}\int_0^{\pi/2} \left(1 + \frac{b\rho_0}{2\sin^2\varphi}\right)^{-P} d\varphi$$

$$= \frac{a\left(1 - \sqrt{\rho_0} g\right)}{2} {}_2F_1\left(\frac{1}{2}, P + \frac{1}{2}; \frac{3}{2}; \frac{-b\rho_0}{2}\right) \quad (8)$$

where $g = \sqrt{\frac{2b}{\pi}} \frac{\left(P - \frac{1}{2}\right)!}{(P-1)!}$ and ${}_2F_1$ denotes the hypergeometric function.

In the case of TX AI and additive receiver noise, which could be an uplink scenario, the SNR ρTX is given by

$$\rho_{TX} = \left[\frac{1}{\rho_t} + \frac{N_t\left[\left(H_n^H H_n\right)^{-1}\right]_{n_t n_t}}{\rho_n}\right]^{-1} = \frac{\rho_t \rho_f}{\rho_t + \rho_f} \quad (9)$$

where, again, ρ_f is distributed according to a chi-squared distribution with 2P degrees of freedom. The probability of error is then computed according to

$$P_e = \int_0^\infty P_{e,M}\left(\frac{\rho_t \rho_f}{\rho_t + \rho_f}\right) p(\rho_f) d\rho_f \quad (10)$$

No general closed form expression for (10) was found. However, for the special cases of low and high SNR ρ_n results were found. These values can serve as bounds on the performance. For low ρ_n, the white Gaussian receiver noise will be dominant in the SNR term ρ_{TX}, which then is well approximated as $\rho_{TX} \approx \rho_n / (N_t[(H_n^H H_n)^{-1}]_{n_t n_t})$. It is clear that ρ_{TX} has a chi-squared distribution with 2P degrees of freedom in this SNR region. Using the findings of Section 3.1, we find that the probability of symbol error then is given by (8), where ρ_0 now equals ρ_n / N_t. For high ρ_n, the TX AI is dominant in the SNR term, which can be approximated as $\rho_{TX} \approx \rho_t$. It is easy to see that the SER is then given by $aQ(\sqrt{p\rho_t})$.

IV. NUMERICAL RESULTS

In this section results from the SER expressions derived in the previous section are first compared with results from Monte-Carlo simulations. As a test case, a MIMO extension of the IEEE 802.11a WLAN standard [7] was studied. The applied parameters are: modulation is 64 QAM, bandwidth is 20 MHz, number of subcarriers N_c = 64, number of carrier used for data transmission is 48, CP length N_g = 16 samples, coding rate is 1. Note that we applied an SNR correction to take into account the loss in signal power by the zero-carriers and CP. Figure 2 shows the results for a 2×4 system experiencing an additive RX impairment, additive white Gaussian receiver noise and a Rayleigh faded channel. It is obvious from Fig. 2 that there is close agreement between the theoretical and simulation results.

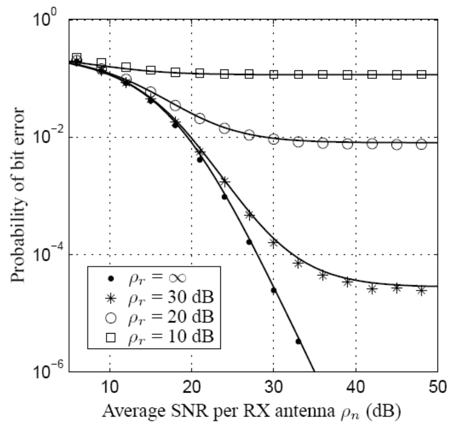

Figure 2: BER for a 2×4 system with RX AI. Theoretical results are depicted with lines and the simulations results by markers.

In Fig. 3 we depict results for a 2×2 system experiencing TX AI. It is clear that there is good agreement between the results from the Monte-Carlo simulations and the theoretical results of (10). Also, the SER in the lower SNR region is well predicted by the lower bound and the error floors agree well with the bounds for high SNR values.

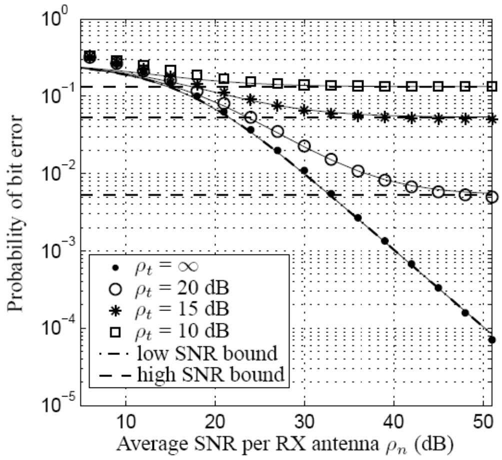

Figure 3: BER for a 2×2 system with TX AI. Simulations results are depicted by markers and the theoretical curves (10) are given by solid lines.

Finally, Fig. 4 shows theoretical results for systems impaired by either TX or RX AI, where the variance of the AI terms is equal for both case, i.e., $\sigma_s^2/100$. It can be concluded that the BER floor introduced by the TX AI does not depend on the number of RX antennas, while it does for the case of RX AI. For a 2×2 setup the influence of the TX AI is greater than that of RX AI, while this is the other way round for the case with 4 and 8 RX branches.

V. CONCLUSIONS

Expressions for the probability of error of an uncoded zero-forcing based MIMO OFDM system with additive TX and RX impairments are derived. Results are given for uncorrelated non-fading as well as Rayleigh fading environments. For the latter case it is shown that the error floor in the case of RX impairments depends on the number of RX antennas, while this is not the case for the TX impairments. The results can serve as a tool for system designers to derive boundaries on the allowed TX and RX impairments to achieve a certain system performance. Furthermore, the results can be used to relate EVM to BER for MIMO systems, under the assumption that the total error term is zero-mean Gaussian distributed. Future research will include the mapping of different radio system impairments on the additive TX/RX noise model and the investigation of the influence of multiplicative error terms.

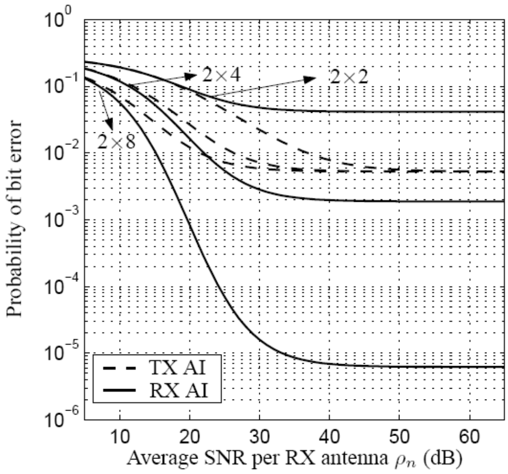

Figure 4: BER for a 2×2, 2×4 and 2×8 system impaired by TX AI or RX AI. Variance of error term is constant.

REFERENCES

[1] B. Come, R. Ness, S. Donnay, L. Van der Perre, W. Eberle, P. Wambacq, M. Engels, and I. Bolsens, "Impact of front-end non-idealities on bit error rate performance of WLAN-OFDM transceivers," in Proc. IEEE Radio and Wireless Conference, 2000,Sept. 2000, pp. 91–94.

[2] R. Hassun, M. Flaherty, R. Matreci, and M. Taylor, "Effective evaluation of link quality using error vector magnitude techniques," in Proc. 1997 Wireless Communications Conference, Aug. 1997, pp. 89–94.

[3] A. van Zelst and T.C.W. Schenk, "Implementation of a MIMO OFDM-based wireless LAN system," IEEE Trans. on Sign. Proc., vol. 52, no. 2, pp. 483–494, Feb. 2004.

[4] J.G. Proakis, Digital Communications, 3rd ed., McGraw-Hill, New York, 1995.

[5] M. Kiessling and J. Speidel, "Analytical performance of MIMO zero-forcing receivers in correlated rayleigh fading environments," in Proc. IEEE Workshop SPAWC 2003, June 2003, pp. 383–387.

[6] M. K. Simon and M.S. Alouni, Digital Communication over Fading Channels, A Unified Approach to Performance Analysis, Wiley, NY, 2000.

[7] IEEE 802.11a standard, ISO/IEC 802-11:1999/Amd 1:2000(E).